Electronic Supplementary Information

Structure and dynamics of double-stranded DNA rotaxanes

Yeonho Song[a] and Jun Soo Kim[a*]

[a]Department of Chemistry and Nanoscience, Ewha Womans University,
Seoul 03760, Republic of Korea

*Corresponding author: jkim@ewha.ac.kr

Contents

Figure S9. Time evolution of the center-of-mass position $z(t)$ of 70-bp-long DNA minicircles over a 2 μs simulation duration.

Figure S10. Time evolution of the center-of-mass position $z(t)$ of 76-bp-long DNA minicircles over a 2 μs simulation duration.

Figure S11. Time evolution of the center-of-mass position $z(t)$ of 82-bp-long DNA minicircles over a 2 μs simulation duration.

Figure S12. Time evolution of the center-of-mass position $z(t)$ of 90-bp-long DNA minicircles over a 2 μs simulation duration.

Figure S13. Time evolution of rotational angle $\phi(t)$ in 70-bp-long DNA minicircles over a 2 μs simulation duration.

Figure S14. Time evolution of rotational angle $\phi(t)$ in 76-bp-long DNA minicircles over a 2 μs simulation duration.

Figure S15. Time evolution of rotational angle $\phi(t)$ in 82-bp-long DNA minicircles over a 2 μs simulation duration.

Figure S16. Time evolution of rotational angle $\phi(t)$ in 90-bp-long DNA minicircles over a 2 μs simulation duration.

Figure S17. Translational mean square displacement (MSD) for DNA minicircles.

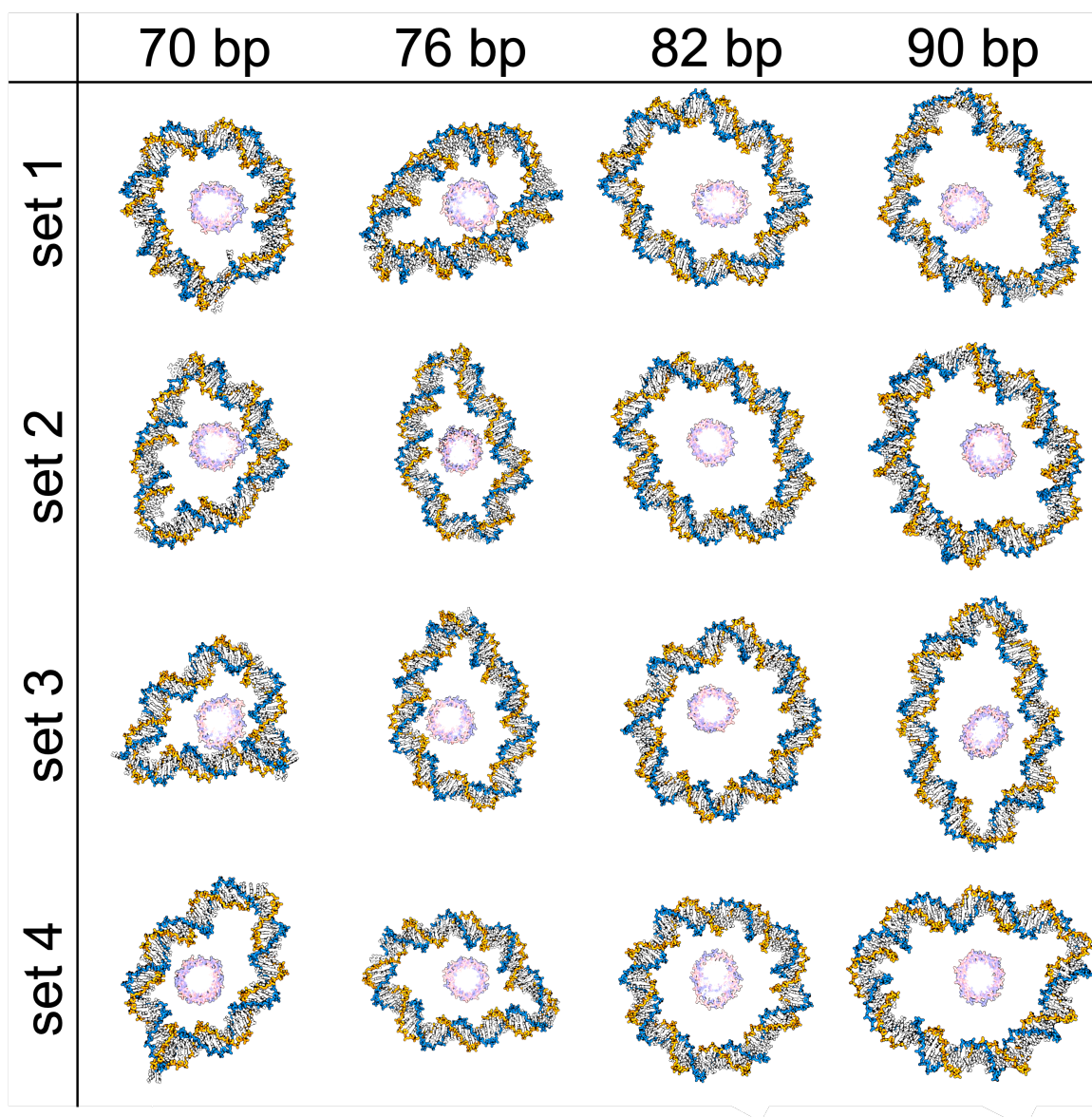**Figure S18.** Rotational mean square angular displacement (MSD) for DNA minicircles.

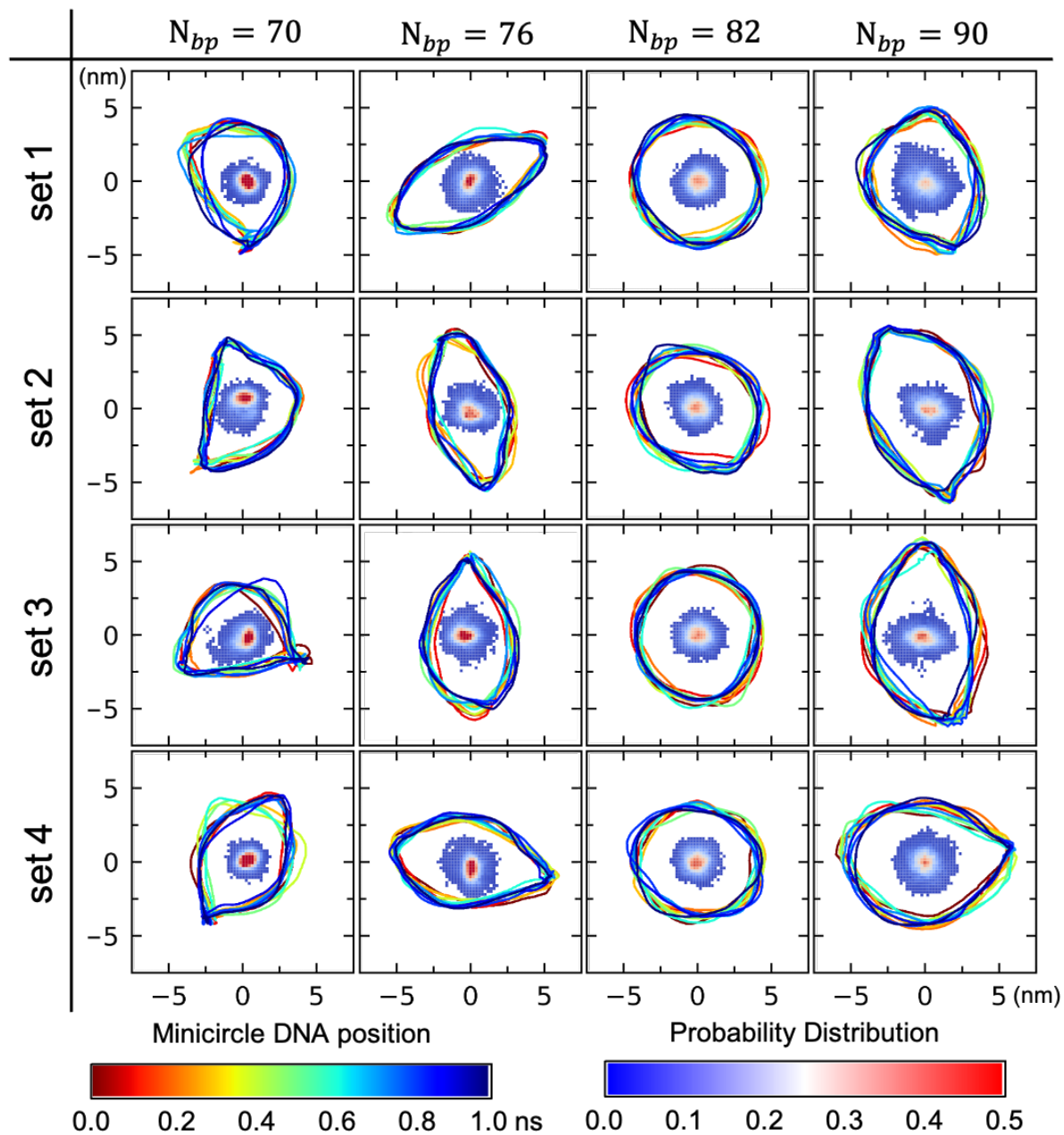**Figure S1. Final snapshots of DNA rotaxane.**

Figure S2. Time evolution of the shape of DNA minicircles. The DNA minicircle shape is visualized through closed curves with varying colors that represent time changes (refer to the upper color bar to the right of the figure for the time sequence), while the probability distribution of the linear DNA axle's position relative to the DNA minicircle is illustrated by the colored dots within each minicircle (refer to the lower color bar to the right of the figure).
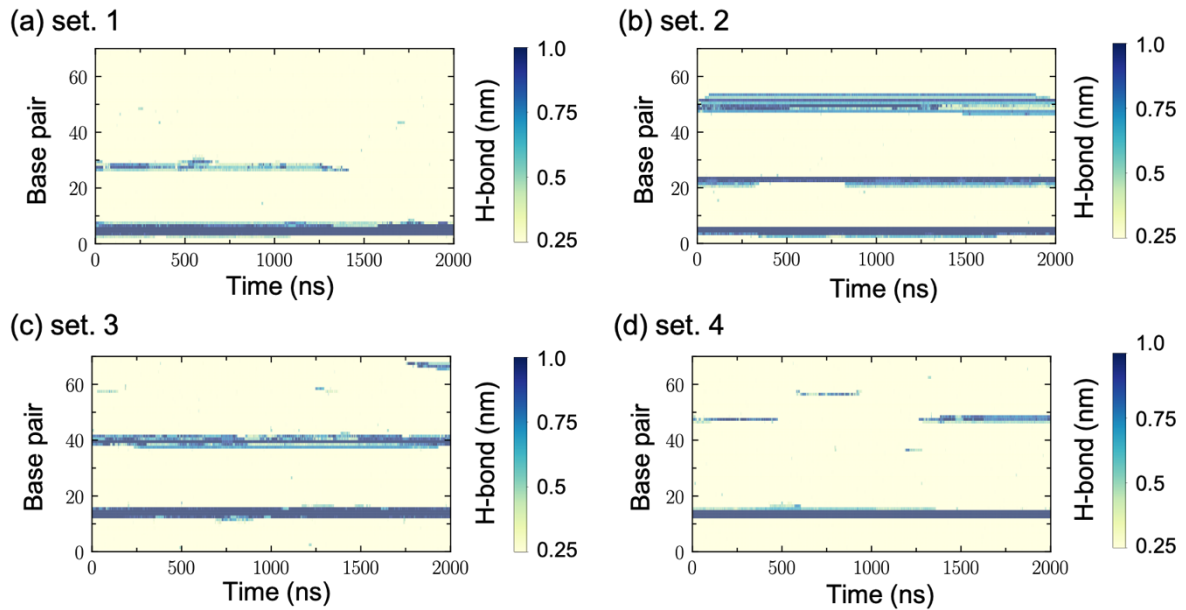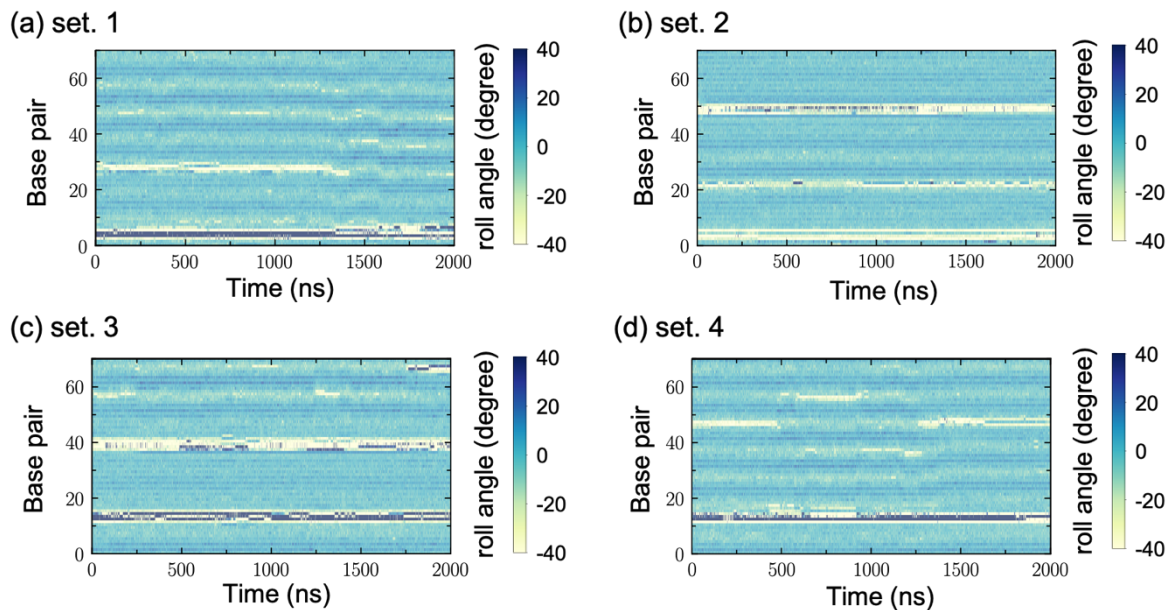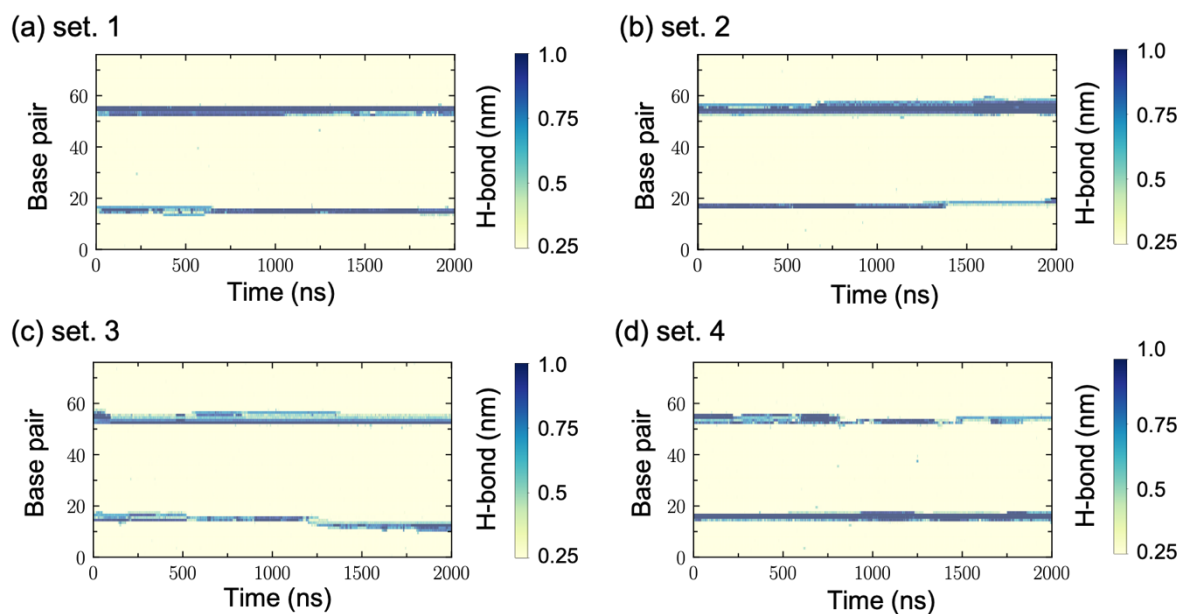
Figure S3. Time evolution of (upper) hydrogen bond distances and (lower) roll angles of all base pairs in 70-bp-long DNA minicircles over a 2 μs simulation duration. Panels (a) to (d) represent four independent simulation sets. Hydrogen bond distances exceeding the range of 0.2-0.4 nm are indicative of base-pair opening, while large negative values of the roll angle are characteristic of kink formation in the DNA structure.
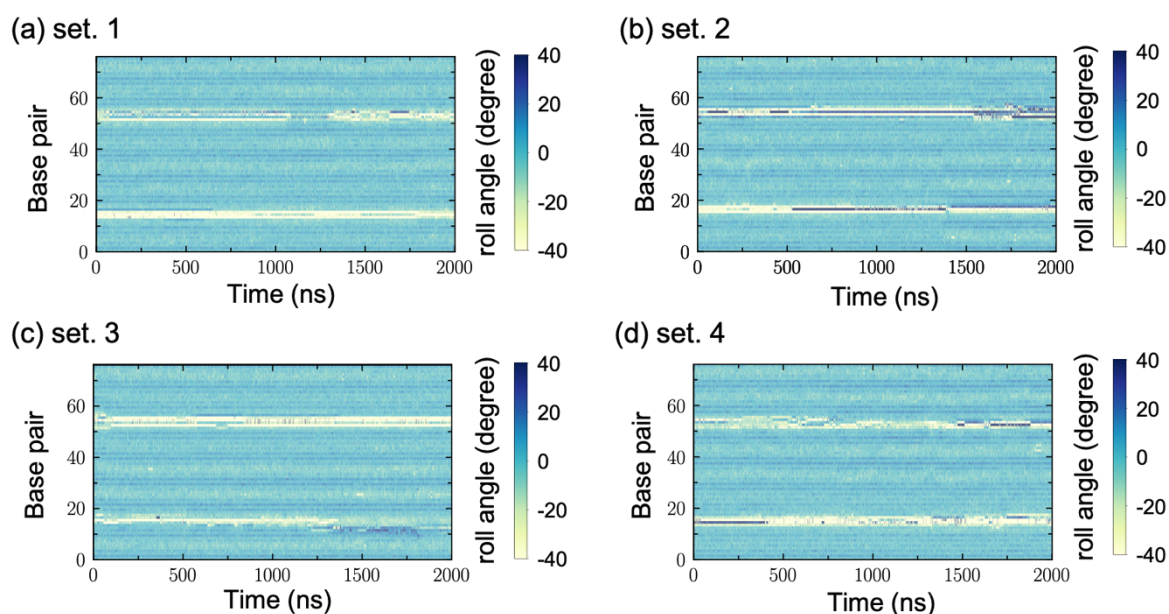
Figure S4. Time evolution of (upper) hydrogen bond distances and (lower) roll angles of all base pairs in 76-bp-long DNA minicircles over a 2 μs simulation duration. Panels (a) to (d) represent four independent simulation sets. Hydrogen bond distances exceeding the range of 0.2-0.4 nm are indicative of base-pair opening, while large negative values of the roll angle are characteristic of kink formation in the DNA structure.

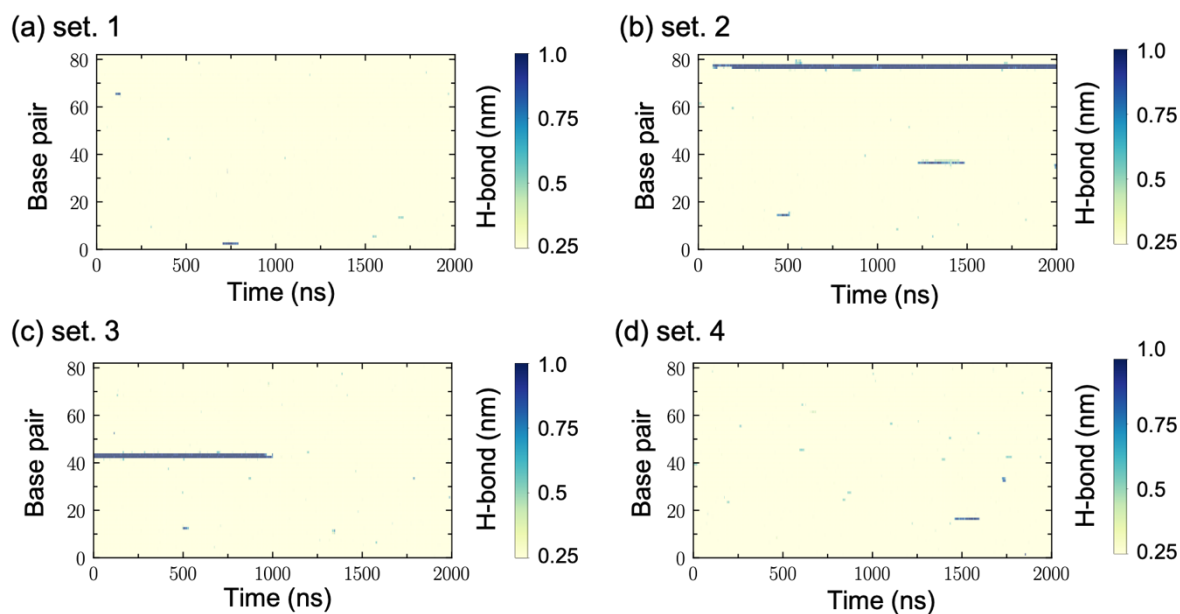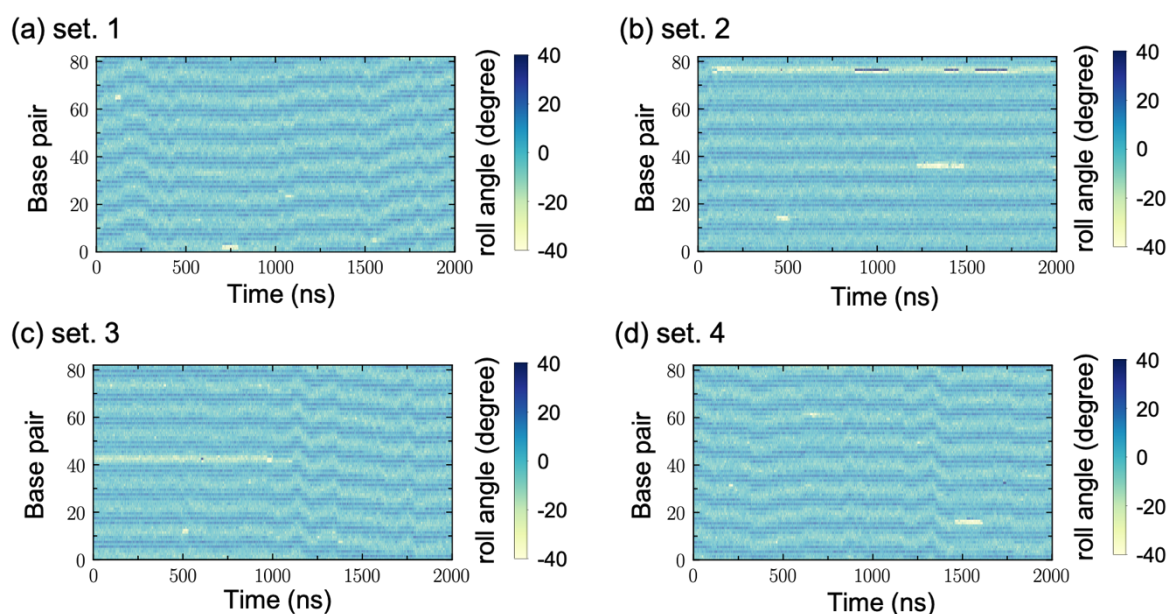**Figure S5. Time evolution of (upper) hydrogen bond distances and (lower) roll angles of all base pairs in 82-bp-long DNA minicircles over a 2 μs simulation duration.** Panels (a) to (d) represent four independent simulation sets. Hydrogen bond distances exceeding the range of 0.2-0.4 nm are indicative of base-pair opening, while large negative values of the roll angle are characteristic of kink formation in the DNA structure.

Hydrogen bond distance: 90 bps

Roll angle: 90 bps

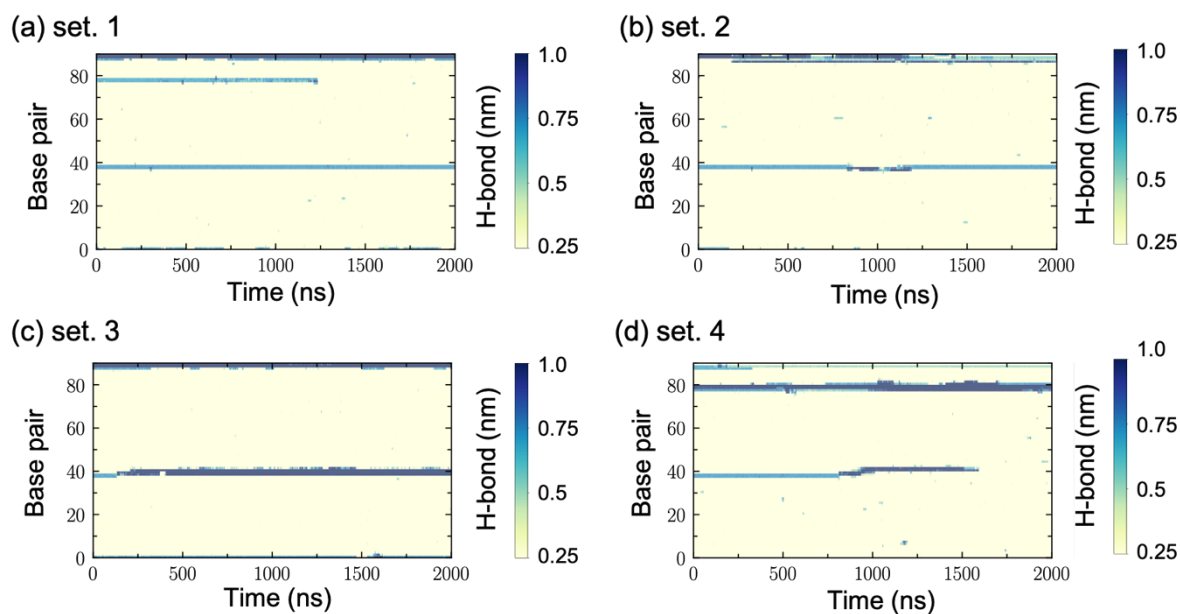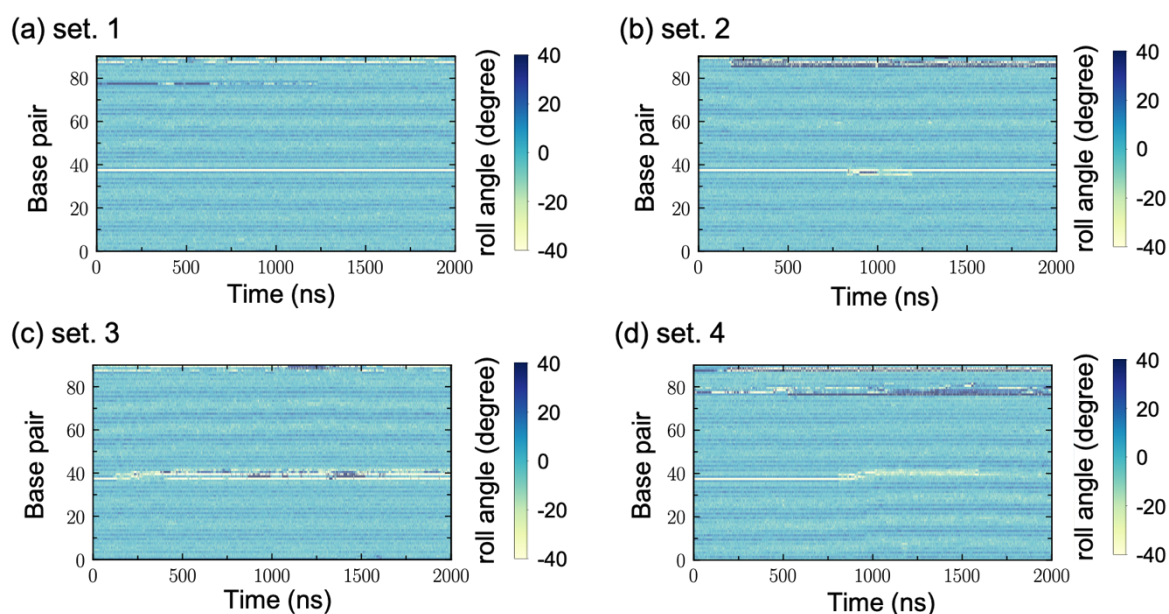**Figure S6. Time evolution of (upper) hydrogen bond distances and (lower) roll angles of all base pairs in 90-bp-long DNA minicircles over a 2 μs simulation duration.** Panels (a) to (d) represent four independent simulation sets. Hydrogen bond distances exceeding the range of 0.2-0.4 nm are indicative of base-pair opening, while large negative values of the roll angle are characteristic of kink formation in the DNA structure.
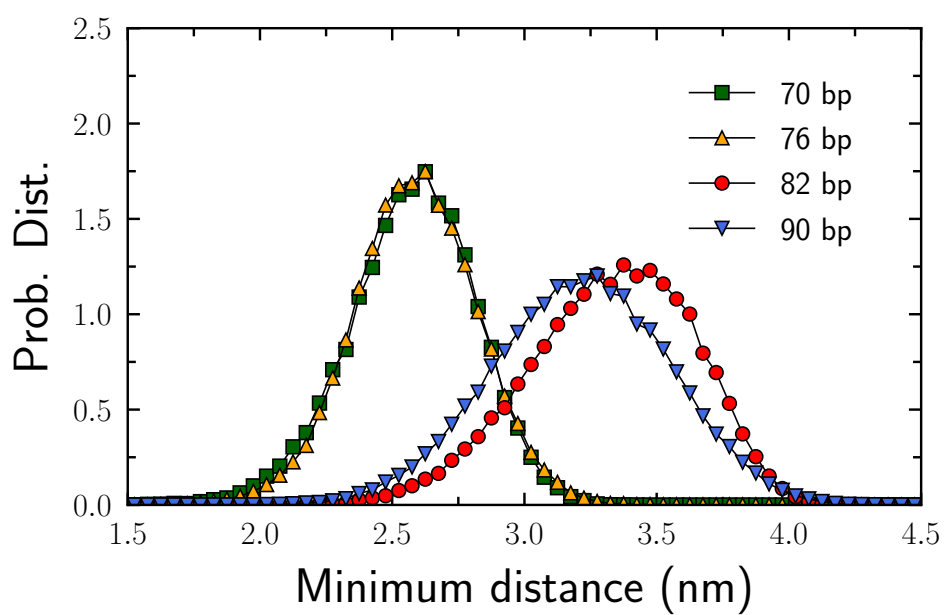
Figure S7. Probability distribution for the minimum distance between circular and linear DNA molecules.
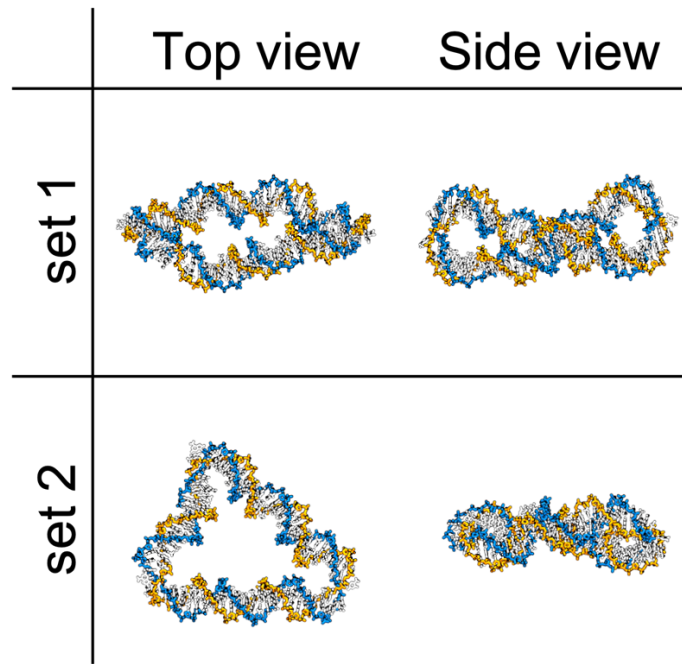
Figure S8. Final snapshots of a DNA minicircle with $N_{bp} = 70$, obtained from the MD simulations of a system containing only a DNA minicircle without a linear DNA axle. The DNA minicircle in the first simulation set is clearly in a supercoiled conformation.

Figure S9. Time evolution of the center-of-mass position $z(t)$ of 70-bp-long DNA minicircles over a 2 μs simulation duration. Panels (a) to (d) represent the results from four independent simulations.

Translation: 76 bps
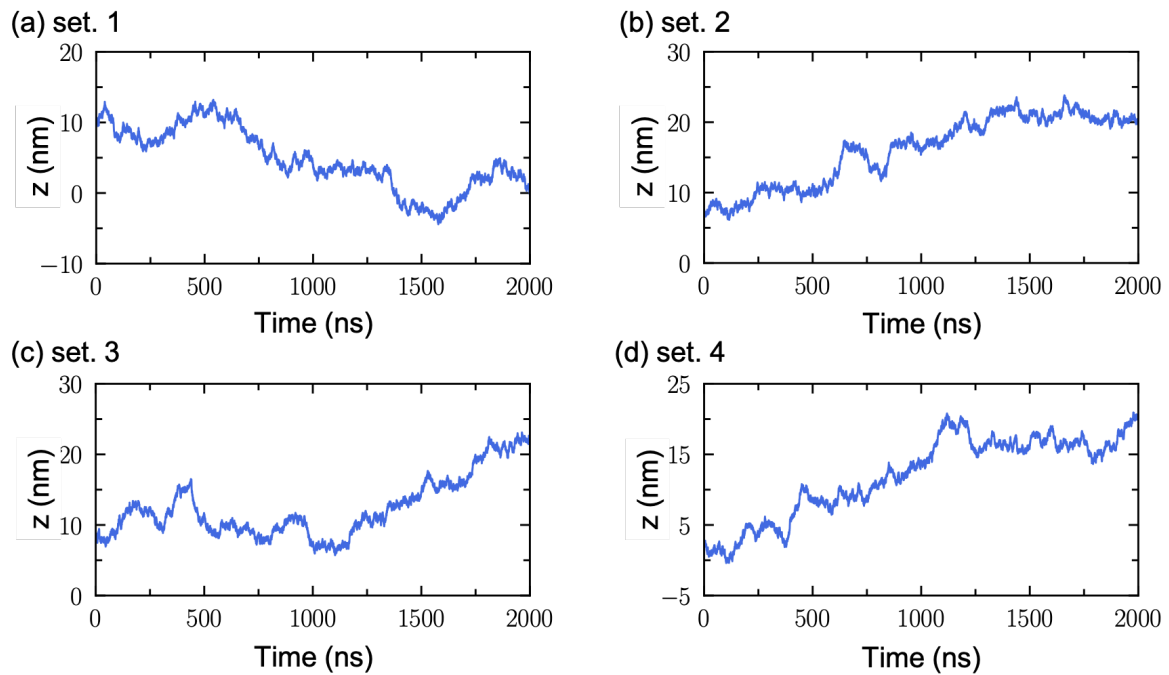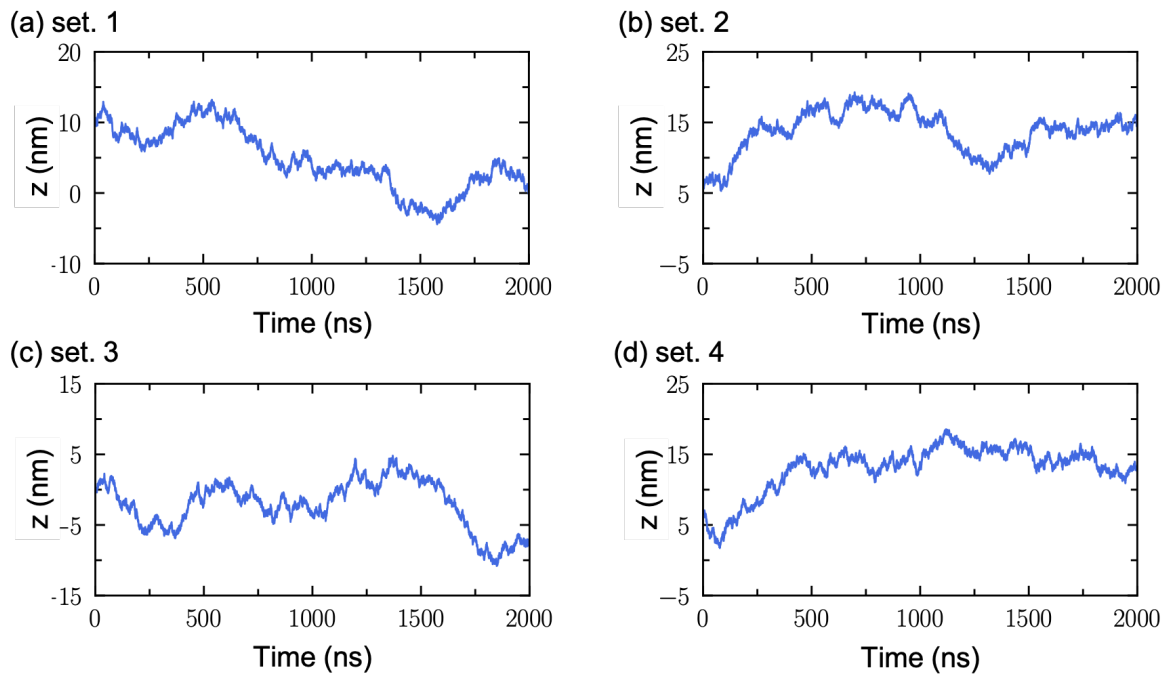
(a) set. 1

(b) set. 2

(c) set. 3

(d) set. 4

Figure S10. Time evolution of the center-of-mass position $z(t)$ of 76-bp-long DNA minicircles over a 2 μs simulation duration. Panels (a) to (d) represent the results from four independent simulations.
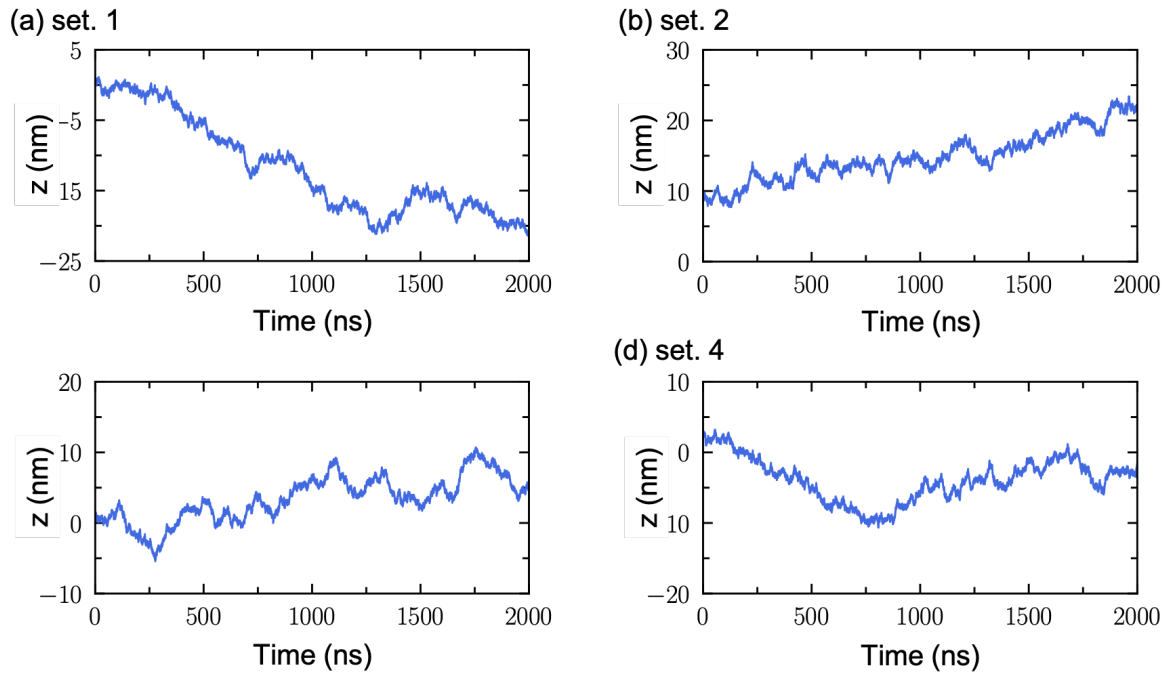
Figure S11. Time evolution of the center-of-mass position $z(t)$ of 82-bp-long DNA minicircles over a 2 μs simulation duration. Panels (a) to (d) represent the results from four independent simulations.
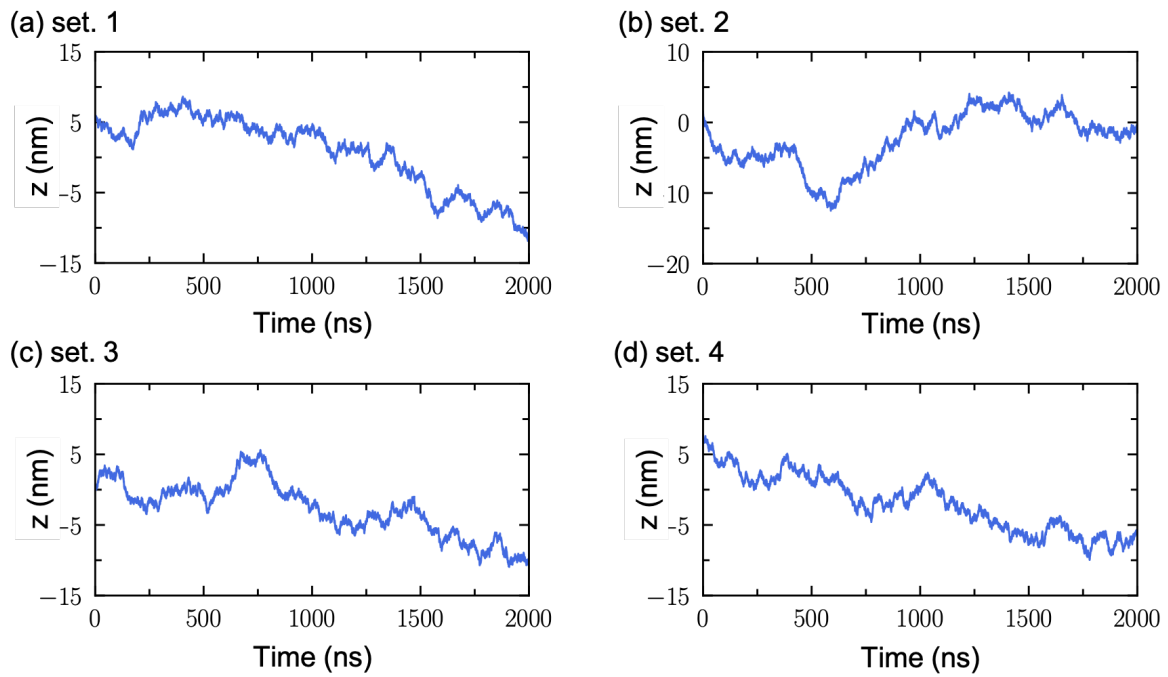
Figure S12. Time evolution of the center-of-mass position of 90-bp-long DNA minicircles, $z(t)$, over a 2 μs simulation duration. Panels (a) to (d) represent the results from four independent simulations.

Figure S13. Time evolution of rotational angle $\phi(t)$ in 70-bp-long DNA minicircles over a 2 μs simulation duration. Panels (a) to (d) represent the results from four independent simulations.
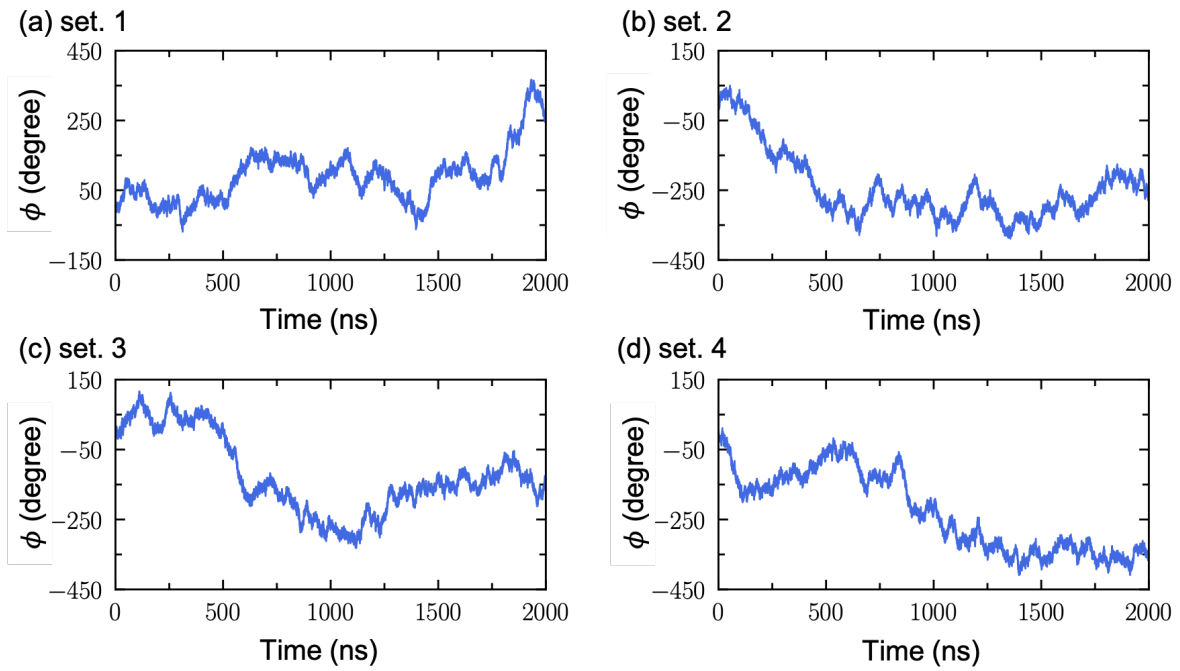
Figure S14. Time evolution of rotational angle $\phi(t)$ in 76-bp-long DNA minicircles over a 2 μs simulation duration. Panels (a) to (d) represent the results from four independent simulations.

Figure S15. Time evolution of rotational angle $\phi(t)$ in 82-bp-long DNA minicircles over a 2 μs simulation duration. Panels (a) to (d) represent the results from four independent simulations.
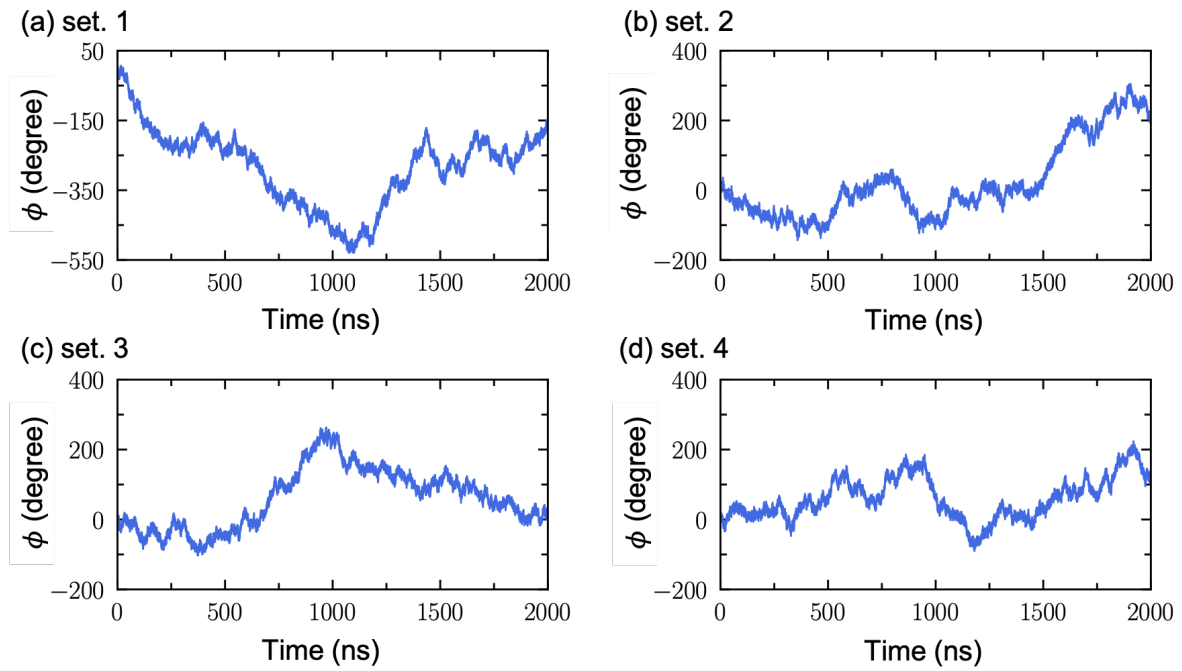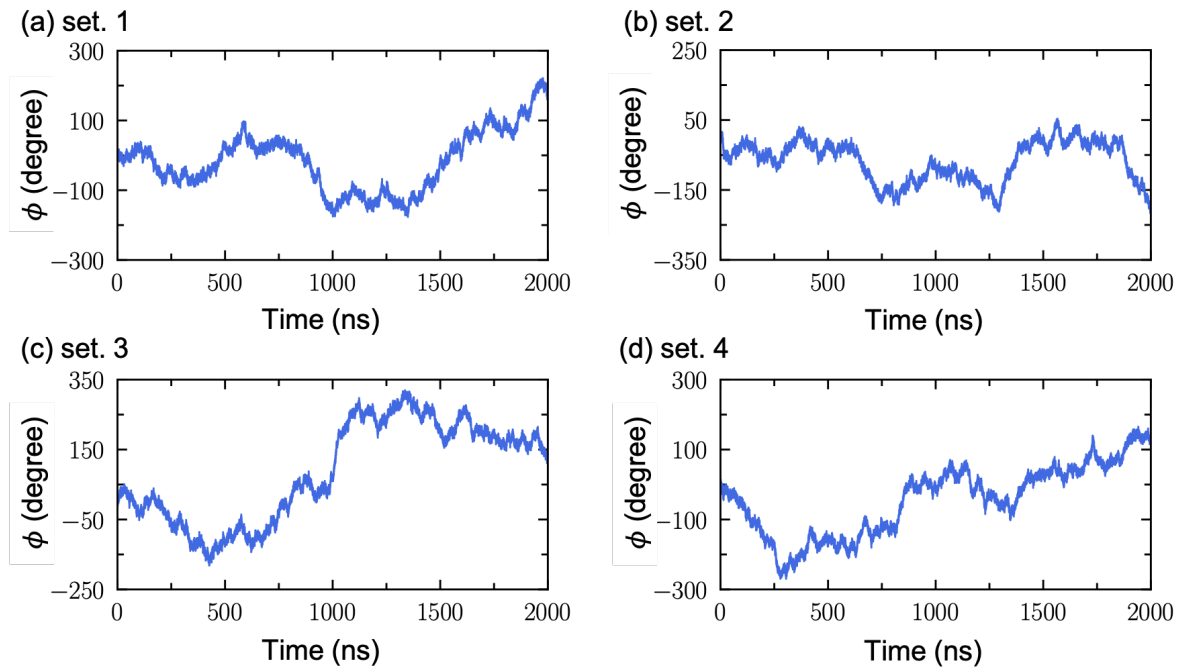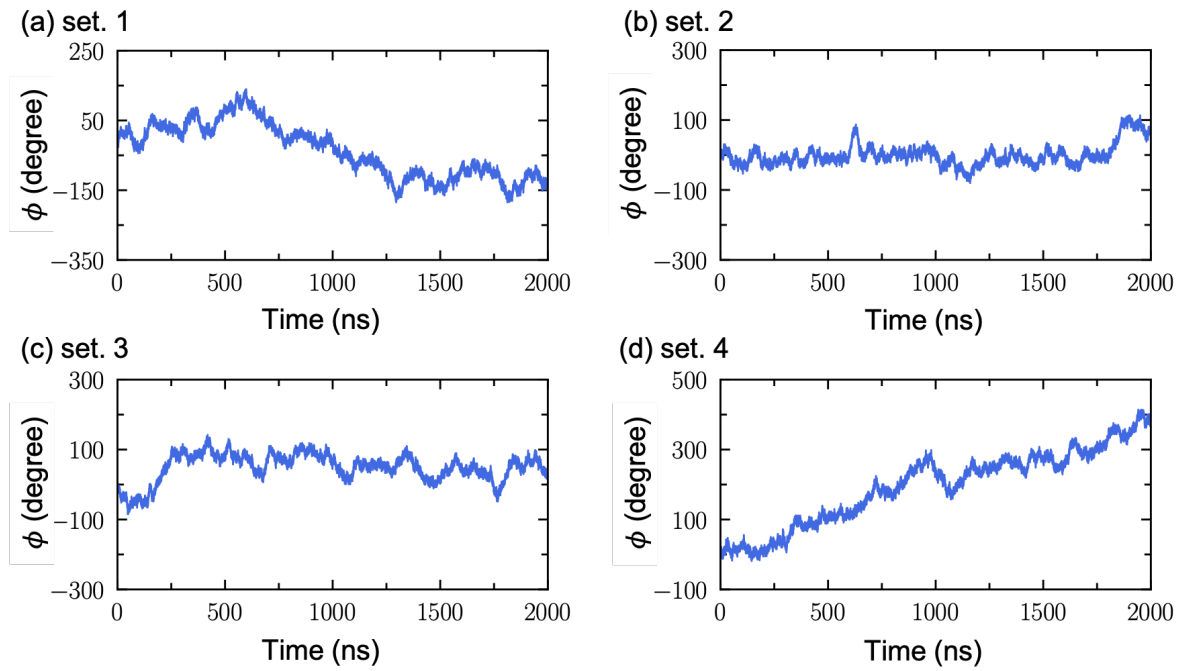
Figure S16. Time evolution of rotational angle $\phi(t)$ in 90-bp-long DNA minicircles over a 2 μs simulation duration. Panels (a) to (d) represent the results from four independent simulations.

Translational MSD

(a) 70 bp

(b) 76 bp
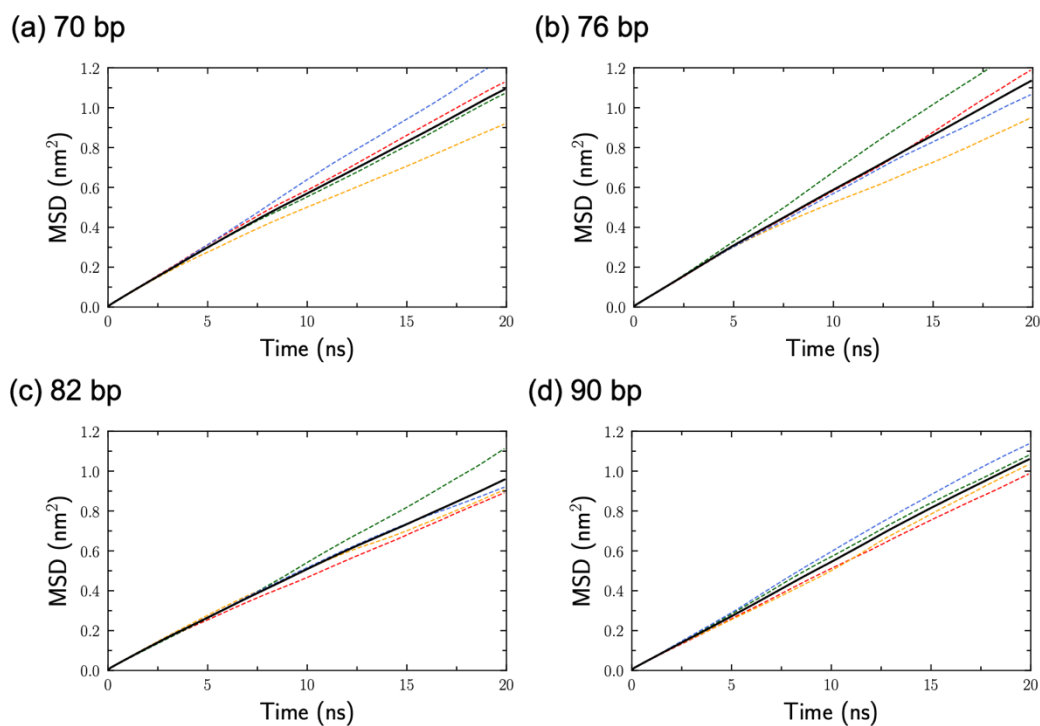
(c) 82 bp

(d) 90 bp

Figure S17. Translational mean square displacement (MSD) for DNA minicircles. The translational MSD was calculated over time as $\langle (z(t) - z(0))^2 \rangle$, where $z(t)$ represents the location of a DNA minicircle along the linear DNA axle at time t. Panels (a), (b), (c), and (d) correspond to N_{bp} values of 70, 76, 82, and 90, respectively. Each panel displays the translational MSD from four independent simulations for each DNA rotaxane (dashed lines). A solid line in each panel corresponds to the addition of all four simulation trajectories, which is presented in Figure 4 of the main text.
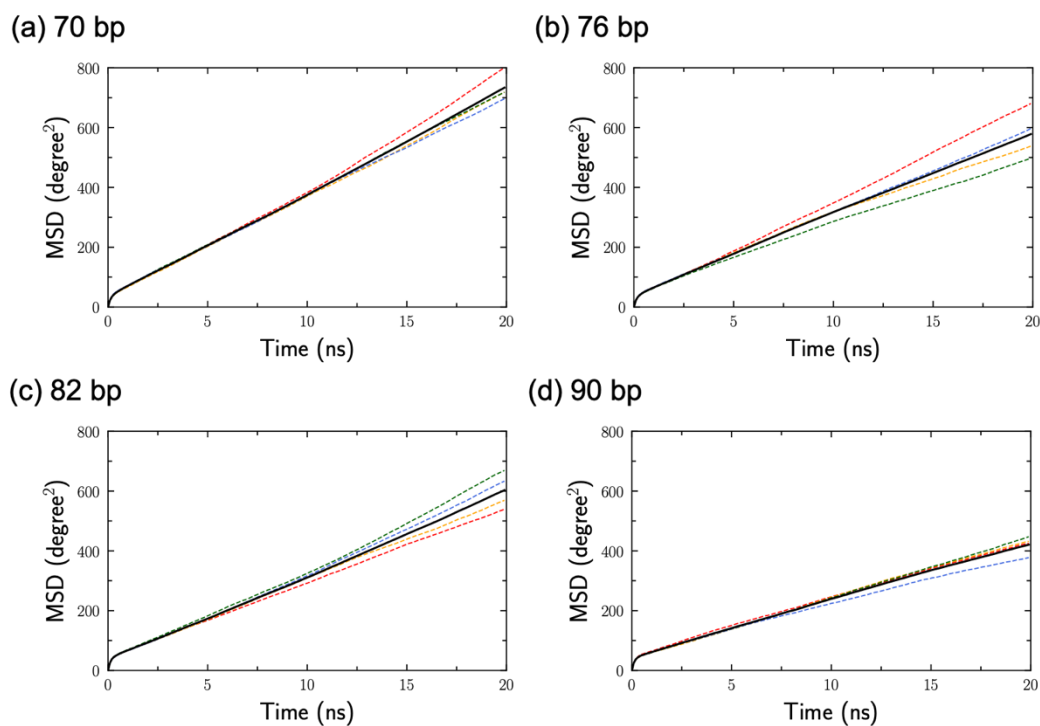
Figure S18. Rotational mean square angular displacement (MSD) for DNA minicircles. The rotational MSD was calculated over time as $\langle (\phi(t) - \phi(0))^2 \rangle$, where $\phi(t)$ is the toroidal angle of a DNA minicircle around the linear DNA axle at time t. Panels (a), (b), (c), and (d) correspond to N_{bp} values of 70, 76, 82, and 90, respectively. Each panel displays the rotational MSD from four independent simulations for each DNA rotaxane (dashed lines). A solid line in each panel corresponds to the addition of all four simulation trajectories, which is presented in Figure 4 of the main text.